Applied Ocean Research 153 (2024) 104287

Contents lists available at ScienceDirect

Applied Ocean Research

journal homepage: www.elsevier.com/locate/apor

Research paper

Fatigue life analysis of threaded connections in offshore wind turbines

Alessandro Annoni [a], Carol Johnston [b], Ali Mehmanparast [a,*]

[a] Department of Naval Architecture, Ocean and Marine Engineering, University of Strathclyde, Glasgow, UK
[b] TWI Ltd, Granta Park, Great Abington, Cambridge, UK

ARTICLE INFO

Keywords:
Threaded connections
Offshore wind
Bolts
Fatigue

ABSTRACT

With the rapid expansion of the installed offshore wind capacity around the world, it is essential to improve the structural integrity of these energy structures for reduced electricity cost and prolonged operational lifespans. An important part of the offshore wind turbine structures is the connection between the monopile foundation and the transition piece. Currently the dominant technology for connecting the monopile to transition piece is using L flanges held together with large-scale bolts. Threaded connections have emerged as a prevalent technology for linking sections of wind turbines, boasting commendable performance despite some inherent drawbacks. This study conducts a comprehensive review of the recommended fatigue design curves for threaded connections in international standards and compares them with the existing fatigue data on medium to large scale bolt sizes. Additionally, the fatigue behaviour of M72 threaded connections has been further analysed by performing new tests with two different values of mean stress. The obtained data from this study have been discussed in terms of the level of conservatism in the recommended fatigue design curves available in international standards for threaded connections. Moreover, the experimental analysis has been combined with numerical and analytical investigations to provide further insight into the life prediction of the threaded connections under fatigue loading conditions.

1. Introduction

Given the escalating threat of global warming to the future of the planet, an internal alliance was established in 2015 to combat climate change by pursuing efforts to restrain the temperature increase below 1.5 °C above pre-industrial levels (Tougher et al., 2017). Following this agreement, several countries, including the UK, have set national targets to achieve net-zero emissions by 2050, underscoring the pressing necessity to address climate impacts. One of the most important sources of clean energy, which is crucial for achieving the pathway to a net-zero target, is offshore wind (HM Government 2020). This form of renewable energy has garnered substantial attention over the past two decades and is experiencing exponential growth worldwide. Offshore wind turbine (OWT) structures generally consist of three main parts, which include: the foundation, transition piece, and tower (see Fig. 1). The foundation connects the structure to the seabed while the transition piece transfers the loads from the tower to the foundation. The dominant majority of the existing OWTs are supported using monopile foundations which are fabricated by forming large-thickness structural steel plates into cylindrical shapes which are subsequently welded in longitudinal and circumferential directions. During the operational phases, the OWT structures are subject to severe cyclic loads coming from the wind, wave and current, which introduce damage into the material. Therefore, engineers and researchers concentrate on diverse facets such as material durability, fatigue damage and environmental effects to refine the design and functionality of the OWT structures. An important area of research which has received a lot of attention in offshore wind industry in recent years is the connection point between the monopile foundation and the transition piece, which is often referred to as MP-TP connection. This is a crucial part of the structure to ensure integrity of the OWT. Hence, a comprehensive engineering analysis is vital to assess fatigue damage and determine the remaining life of this part of the OWT structure.

The first MP-TP connection technology utilised in OWTs was the grouted connection, which has been historically employed in the offshore Oil and Gas foundation piles. This design employs a tube-in-tube connection with the space between filled with the grout (Mehmanparast et al., 2020). Load transfer primarily occurs through shear friction induced by normal stress from surface imperfections and roughness, as well as compression of the grout. However, in 2009 many of the MP-TP grouted connections in various offshore wind farms were

* Corresponding author.
E-mail address: ali.mehmanparast@strath.ac.uk (A. Mehmanparast).

https://doi.org/10.1016/j.apor.2024.104287
Received 17 July 2024; Received in revised form 12 September 2024; Accepted 21 October 2024
Available online 31 October 2024

Nomenclature

A	Cross sectional area
A_f	Fast fracture area
F_{max}	Maximum load
F_{min}	Minimum load
$log\ a$	Intercept of mean S-N curve
$log\ \bar{a}$ (or $logC_d$)	Intercept of design S-N curve
m	S-N curve inverse slope
R^2	Coefficient of determination
$R_{p,0.2,nom}$	0.2 % proof stress (often taken as the yield stress)
S_A	Stress amplitude
S_L	Fatigue endurance limit
S_m	Mean stress in a fatigue cycle
S_{max}	Maximum stress in a fatigue cycle
S_{min}	Minimum stress in a fatigue cycle
S_r (or S)	Stress range in a fatigue cycle
S_{UTS} (or UTS)	Ultimate tensile strength
BL	Black (i.e. uncoated) bolts
HTG	High temperature galvanised bolts
MP-TP	Monopile-Transition piece connection
NTG	Normal temperature galvanised bolts
OWT	Offshore wind turbine
SCF	Stress concentration factor
SD	Standard deviation
YS	Yield stress

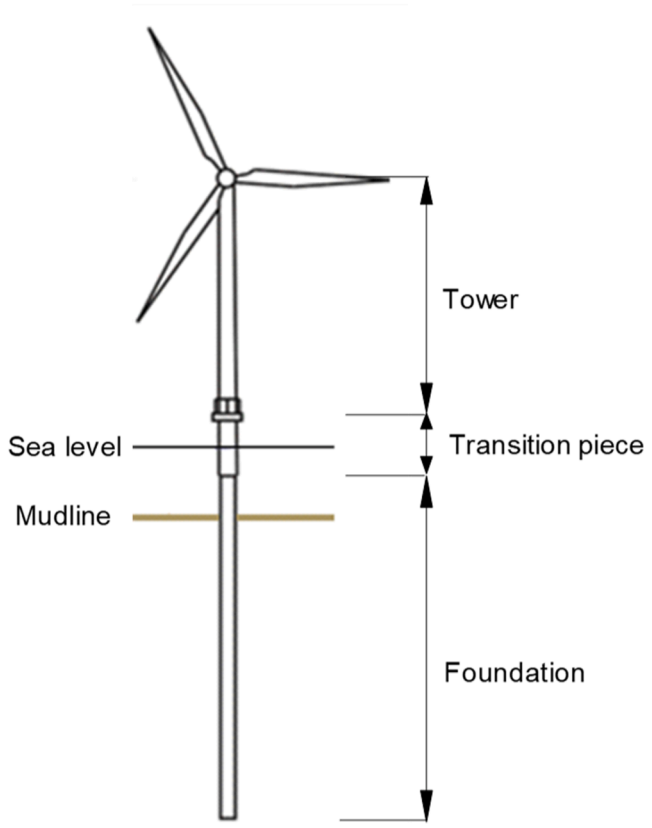

Fig. 1. A typical layout of an OWT.

observed to be failing. The absence of shear keys on straight MP and TP surfaces was identified as a key issue resulting in failure of the grouted connections. Moreover, the bending load complexity in offshore wind structures, compared to Oil & Gas structures, and the impact of wave loading were not adequately considered during the design phase of MP-TP grouted connections. Additionally, the axial capacity of the connection was found to be significantly lower than the assumed level during scaled tests, with manufacturing and installation tolerances exacerbating bending stress (Lotsberg et al., 2012). Common failure modes of the grouted connection included dis-bonding, cracking, wear, and compressive grout crushing failure (Redondo and Mehmanparast, 2020).

Following the grout failures in OWTs, the alternative solutions for MP-TP connection were investigated and since then bolted flange connections have been widely used to connect the monopile to the transition piece in OWTs. This technology has been successfully used in the offshore Oil&Gas industry for decades, therefore it was chosen as a reliable substitute for the grouted connection in MP-TP connections. In the offshore wind industry, the employment of this connection technology is based on the presence of two L-flanges circumferentially welded onto two tubular sections and held together using a series of bolts (Seidel and Schaumann, 2001). Over the past decade, with the increase in the wind turbine size and capacity, the size of the OWT foundations has also increased accordingly. As a result of scaling up the OWT geometries, the size of the threaded bolted connections has also increased significantly. In the MP-TP connection of OWTs the number of bolts around the circumference of the flange depends on a number of factors such as the radius and thickness of the flange, the size of the bolt and the operational loading condition. In order to introduce the required level of clamping force, nuts which are often accompanied by washers are tightened on the bolts to create a pre-tension that keeps the MP-TP flanges together, and also protect the bolts against fatigue loads. While torquing is often employed in tightening of the smaller bolts and nuts, the pre-tensioning method is widely used in large-scale OWT bolted connections. In this approach, the bolt is elastically stretched while the nut is positioned on the threads and once the tensile pressure on the bolt is released a pre-load is formed in the threaded connection. It has been shown in the literature that the level of pre-load in individual bolts is very sensitive to the tightening sequence (Braithwaite and Mehmanparast, 2019). Moreover, it has been shown in the literature that the pre-load level reduces after tightening as a result of embedment during the tightening process, time-dependent creep deformation of the material and also the cyclic loading condition experienced by the OWTs (Braithwaite et al., 2020). Due to the relaxation of the pre-load in MP-TP bolted flange connections, frequent inspections need to be carried out to measure the pre-tensioning force in bolt and nut connections and tighten or replace those with reduced levels of pre-load.

The bolted joints in MP-TP connections of OWTs are subject to cyclic loads during their operational lifespan which introduce fatigue damage in the threaded connections. Fatigue failure of bolts typically occurs in the first few engaged threads between the bolt and the nut which have the highest values of stress concentration factor (SCF). According to the data in the literature, 65 % of fatigue failures in bolted connections occur in the root of the first engaged thread, 20 % in the thread run-out region and 15 % in the head to shank radius (Charlton, 2011; Stranghöner et al., 2018) (see Fig. 2). Considering that fatigue damage is the dominant failure mechanism in OWT bolted connections, appropriate fatigue design curves available in international codes and standards must be employed in the design process. While similar approaches are used in all of the international standards for design against fatigue failure, there are differences in fatigue Class depending on manufacturing method (heat treatment, rolled versus cut threads) of threaded connections and the thickness correction for the fatigue design curves are different. The effect of these differences needs to be

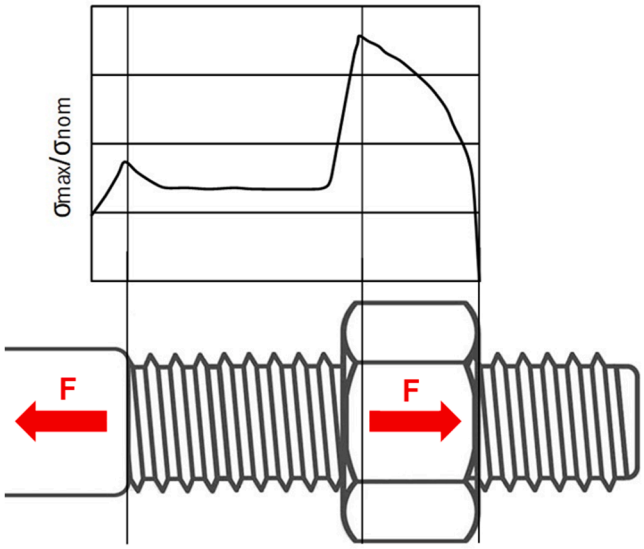

Fig. 2. Schematic illustration of stress distribution in a threaded connection under pre-load, F (re-produced based on the information presented in (Stranghöner et al., 2018)).

understood in the design and analysis of MP-TP bolted connections (Johnston and Doré, 2021; Lochan et al., 2019).

In this paper, the existing fatigue data points available in the literature for various medium to large scale bolt sizes (M36, M48, M64 and M72) and heat treatments have been collated and analysed, and the results are compared with the design curves recommended in international standards to examine the accuracy of thickness correction factors for a range of bolt sizes examined in this study. Moreover, due to the limited availability of fatigue data points on M72 bolts, which are widely used in MP-TP connections of the existing OWTs in the UK and Europe, new fatigue experiments have been conducted on M72 threaded connections under two different mean stress levels and the Goodman analysis has been employed for accurate interpretation of the test results. The results obtained from this study have been discussed in terms of the level of conservatism with respect to the existing fatigue design curves particularly when the existing thickness correction factors are employed to design larger bolts in MP-TP connection of OWTs.

2. Analysis of the existing fatigue data on medium to large scale bolts

2.1. A summary of main parameters in fatigue design curves

In order to design MP-TP bolted flange connections for OWTs, where cyclic loads are constantly applied on the structure, the fatigue design curves (which are often referred to as S-N curves) are commonly employed in engineering analyses. There are three main codes and standards which are often used for design of threaded connections against fatigue failure: Eurocode 3 EN 1993–1–9:2005 (EN 1993-1-9 2005), DNV–RP-C203 (DNV-RP-C203 2021) and the BS 7608 (BS 7608 2015). The general form of the S-N fatigue design curve is presented in Eq. (1), where N is the number of cycles to failure, $\Delta\sigma$ (or S or S_r) is the stress range in MPa, $\log\bar{a}$ is the intercept (which is equivalent to $\log C_d$ in BS 7608) of the design curve and m is the inverse slope of the S-N curve in log-log axes.

$$\log N = \log\bar{a} - m\log\Delta\sigma \quad (1)$$

In Eq. (1), $\log\bar{a}$ can be obtained by subtracting from intercept of the mean line $\log a$ two standard deviations (SD or $s_{\log N}$), which corresponds to the lower bound 97.7 % survival probability, following this equation:

$$\log\bar{a} = \log a - 2s_{\log N} \quad (2)$$

The comparison of the S-N curves in these standards shows that for a given class of fatigue design, the change in inverse slopes (m) occurs at different number of cycles depending on which standard is followed. Moreover, in the case of threaded connections different considerations have been made in terms of the heat treatment and the manufacturing process in each of the threaded fastener fatigue classes. For large scale bolts the standards provide a mathematical scaling of the curves, based on an empirical equation which depends on the reference thickness t_{ref} (which is 25 mm according to DNV-RP-C203 and BS 7608 standards and 30 mm according to Eurocode), the actual thickness t (or diameter of the bolt), and the thickness correction exponent k (which is equivalent to b in BS 7608, and is equal to 0.25 for threaded connections subjected to stress variation in the axial direction).

2.2. Fatigue data on medium to large scale bolts

The existing fatigue data points from the tests on medium to large scale bolts under axial loading condition have been collated from the open literature and re-analysed in this study. A review of the collected literature data shows that with increasing the bolt size, the number of existing data points significantly reduces due to the need to access higher load carrying capacity machines and higher associated costs for operating the tests on larger bolts. Four bolt sizes have been considered in this study which include M36, M48, M64 and M72. The results obtained from the fatigue analysis on the collected data points on these bolt sizes are compared with the recommended design curves from the three main international standards mentioned above. All of the fatigue data points considered in this study were obtained from the tests in air, and the influence of free-corrosion environment on the fatigue life of threaded connections is not considered in this study. Moreover, the data points considered in this study were obtained from the tests continued until failure and the run-outs were excluded.

The fatigue data were collected from (Mang et al., 2003; Schaumann et al., 2015; Schaumann and Eichstädt, 2016; Schaumann and Eichstädt, 2018) for M36 bolts, (Schaumann, 2009; Unglaub et al., 2015) for M48 bolts, (Johnston and Doré, 2021; Schaumann and Eichstädt, 2016; Schaumann and Eichstädt, 2018) for M64 bolts and (Johnston and Doré, 2021) for M72 bolts, and the results obtained from the linear regression analyses are presented in Fig. 3(a), (b), (c) and (d), respectively. Also included in these figures are the comparison of the data points with the thickness corrected standard fatigue design curves of Class FAT 50 from Eurocode 3 EN 1993–1–9:2005 for galvanised threads (EN 1993-1-9 2005), Class G from DNV–RP-C203 for hot galvanised threads (DNV-RP-C203 2021) and Class X-20 % from the BS 7608 for galvanised threads (BS 7608 2015). Different surface treatments were considered in the analysis which include black or uncoated (BL) bolts (presented in black symbols), normal temperature (NTG) (presented in blue symbols) and high temperature (HTG) hot-dip galvanised bolts (presented in red symbols). It is worth noting that due to the corrosive environments in offshore applications, the bolts are often galvanised for corrosion resistance purposes; however, some data are available on uncoated (i.e. black) bolts in the literature to evaluate the influence of galvanisation process on the fatigue life of bolted connections. For each of the fatigue data sets, a regression analysis in log-log scale was carried out, to find the lower bound 97.7 % survival probability line, and the corresponding parameters were quantified for M36, M48, M64 and M72 bolt sizes which are summarised in Table 1. This table shows the results of the inverse slope m, standard deviation, the intercept of the mean-2SD line $\log\bar{a}$, and the coefficient of determination R^2 for different bolt sizes and surface treatments.

As seen in Fig. 3, the data points from the literature for M36 bolts were classified in BL, NTG and HTG subsets, whereas the data points found for M48 and M72 were on galvanised bolts and the data points on

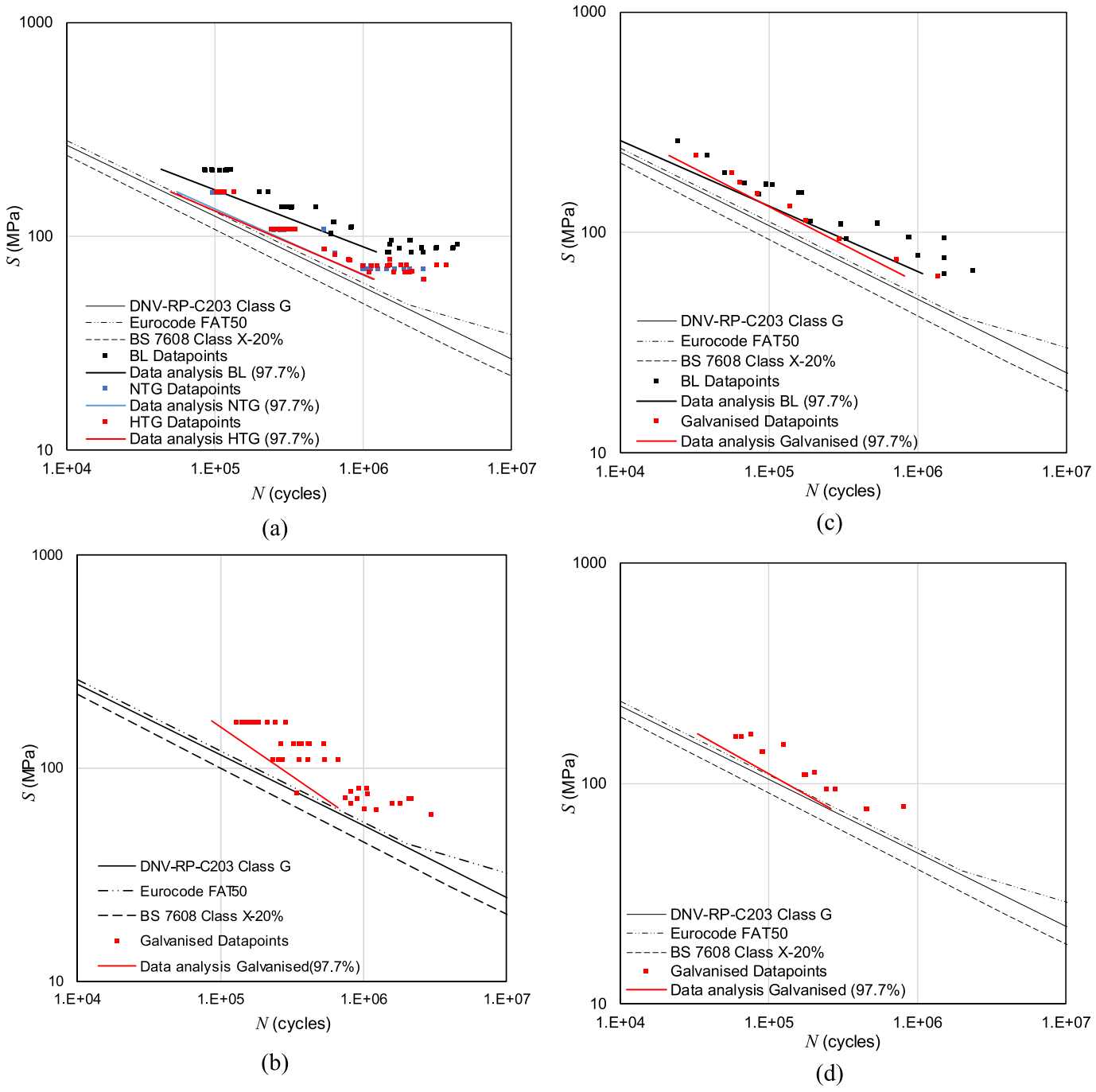

Fig. 3. Comparison of fatigue data points with different surface treatments for (a) M36, (b), M48, (c) M64, and (d) M72 bolt sizes, with the thickness corrected fatigue design curves from various standards.

Table 1
Lower bound 97.7 % survival probability regression analysis results for various bolt sizes.

	M36			M48	M64		M72
	BL	NTG	HTG	Galvanised	BL	Galvanised	Galvanised
m	3.75	3.23	3.36	2.16	3.37	2.89	2.66
$log\,\bar{a}$	13.315	11.881	12.121	9.733	12.153	11.130	10.429
SD	0.155	0.111	0.140	0.165	0.158	0.066	0.146
R^2	0.923	0.945	0.921	0.796	0.925	0.987	0.931

M64 were the combination of BL and galvanised bolts. As seen in Fig. 3 and Table 1, the inverse slope of the S-N curve obtained from the literature data points on various bolts sizes fluctuates above and below $m = 3$, which is the recommended inverse slope by all standards for low and medium cycle fatigue. Also seen in Fig. 3 and Table 1 is that the intercept of the S-N curve corresponding to 97.7 % survival probability

($\log \bar{a}$) and also the inverse slope of m are lower in galvanised M36 and M64 bolts compared to the black bolts. As discussed in (Johnston and Doré, 2021; Schaumann and Eichstädt, 2018; Ungermann et al., 2015), while the galvanised bolts show a better resistance to corrosion in seawater with cathodic protection, in the air condition they generally reduce the fatigue life compared to the uncoated bolts.

It can be seen in Fig. 3 that except for one data point from a galvanised M48 bolt, the rest of the experimental fatigue data points obtained from the range of bolt sizes considered in this study fall above the thickness corrected fatigue design curves recommended by all three standards for galvanised threaded connections. Finally seen in Fig. 3 and Table 1 is that the lower bounds (i.e. mean-2SD) obtained from regression analyses on galvanised bolts generally fall upon or above thickness corrected Class FAT 50 from Eurocode 3 EN 1993–1–9:2005 (EN 1993-1-9 2005), while the recommended thickness corrected fatigue design curves of Class G from DNV–RP-C203 (DNV-RP-C203 2021) and Class X-20 % from the BS 7608 (BS 7608 2015) standards may underpredict the fatigue life at some of the stress range values for various bolt sizes examined in this study. The comparison of the recommended design curves shows that while all three standards suggest the same inverse slope of $m = 3$ for the low and intermediate cycle regions, the most and the least conservative design lives are obtained from Class X-20 % of BS 7608 and Class FAT 50 of Eurocode, respectively, with the recommended fatigue design curve from Class G in DNV-RP-C203 falling in between these two. The lower level of conservatism in thickness corrected Class FAT 50 of Eurocode standard can be associated with the higher reference thickness (i.e. diameter) value of 30 mm in thickness correction calculations recommended by Eurocode compared to the value of 25 mm employed in DNV-RP-C203 and BS 7608 standards.

3. New fatigue tests on M72 threaded connections

Although M72 bolts made of grade 10.9 steel are widely used in MP-TP connections of fixed-bottom OWTs in the UK and Europe, it is evident from Fig. 3(d) that there is a limited number of fatigue data points available in the open literature on this thread size. This is presumably due to the fact that the performance of fatigue tests on large-scale threaded connections is relatively expensive because of the material costs, the operational costs of the fatigue test machines with high load carrying capacities, and relatively low frequencies in large-scale testing which make the tests very time consuming. In order to further investigate the fatigue behaviour of M72 threaded connections under tensile loading conditions and to improve the design and integrity assessment of bolted flange MP-TP connections, seven new fatigue tests, denoted M01—M07, were carried out in this study on hot-dip galvanised M72 studs and the results from these tests are presented below.

3.1. Test set up and loading condition

Fatigue tests were performed at TWI using servo-hydraulic test machines with load carrying capacity of 1000 kN and 2500kN. An example of a fatigue test on a servo-hydraulic machine is demonstrated in Fig. 4. The fatigue tests were performed under constant amplitude loading condition with uniaxial loading direction, and two distinct nominal mean stress S_m values were applied in these new experiments. Five tests were performed under the mean stress of $S_m = 202$ MPa with another two tests under $S_m = 624$ MPa. For each of the mean stress values considered in this study, various values of stress range were implemented in different tests to build a new knowledge on the fatigue performance of MP-TP threaded connections. All tests were run at 1 Hz frequency and continued until the failure was occurred in the threaded connections. The values of maximum stress S_{max}, minimum stress S_{min}, stress range S_r (or S, which is the difference between S_{max} and S_{min}) and mean stress S_m are reported in Table 2 for each of the new tests performed in this study.

3.2. Test results

The new M72 test data obtained from this study were analysed by conducting linear regression analyses on 5 data points with the mean stress of $S_m = 202$ MPa, two data points with the mean stress of $S_m = 624$ MPa, and seven data points with the combined mean stresses of 202 MPa and 624 MPa, and the results are shown in Table 3. The mean curve obtained from the regression analysis on all new data points together with the upper bound of mean+2SD and lower bound of mean-2SD are

Table 2
Fatigue loading condition for each of the new tests performed on M72 studs.

	S_{max} (MPa)	S_{min} (MPa)	S_r (MPa)	S_m (MPa)
M01	281	124	157	202
M02	270	134	136	202
M03	257	147	110	202
M04	272	132	140	202
M05	249	155	94	202
M06	679	568	111	624
M07	694	553	141	624

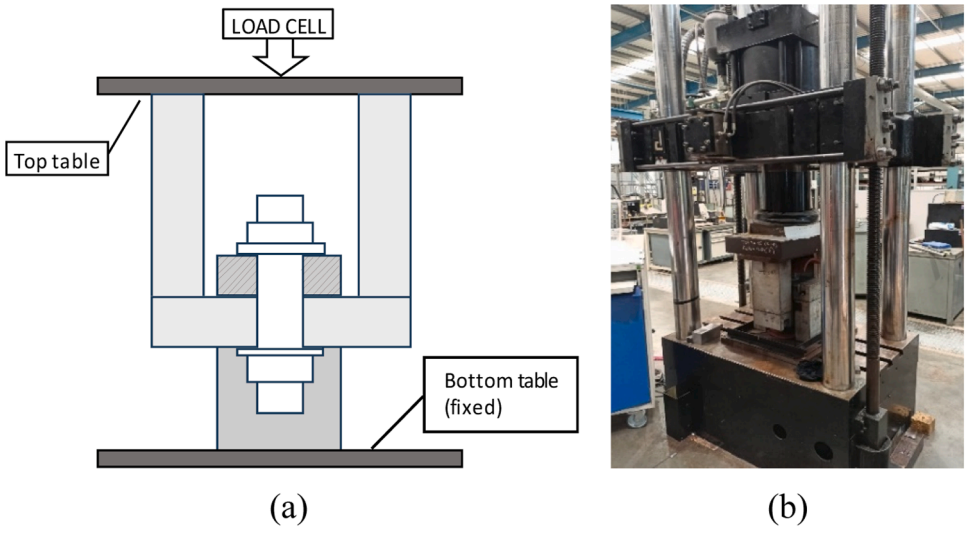

Fig. 4. (a) Schematic set up of the fatigue tests on M72 studs, (b) a picture of the fatigue test set up on a servo-hydraulic machine.

Table 3
A summary of data analysis results from the new data set and combination of the literature data and new data on M72 threaded connections.

	New data (S_m=202 MPa)	New data (S_m=624 MPa)	All new data	Combined literature and new data
m	1.85	2.95	2.00	2.32
$log\ \bar{a}$	9.064	–	9.384	9.727
SD	0.191	–	0.167	0.214
R^2	0.499	1.000	0.516	0.607

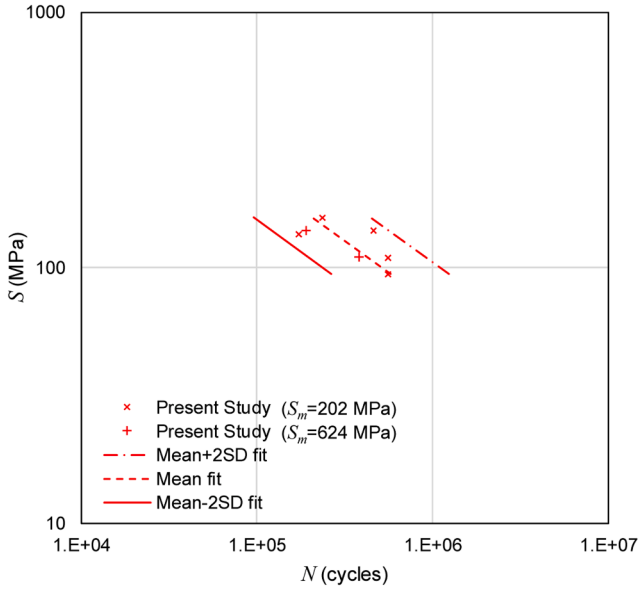

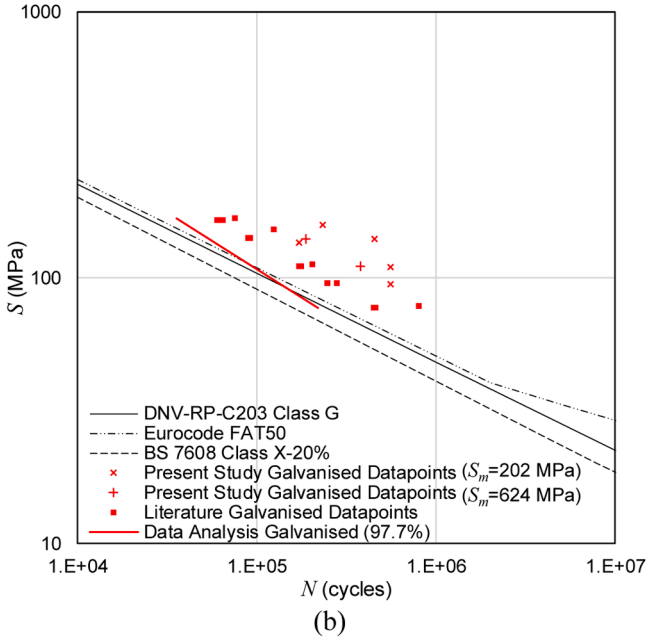

Fig. 5. (a) Regression analysis on all new M72 fatigue data points presented in this study, (b) Regression analysis on the combined literature and new data sets on M72 threaded connections, compared with thickness corrected fatigue design curves recommended by various standards.

shown in Fig. 5(a). Moreover, further regression analysis was conducted on the combination of the existing M72 data points available in the literature (see Fig. 3(d)) and the new test data obtained from the present study (i.e. seven new tests on M72 studs), and the results are shown in Fig. 5(b). Following the S-N relationship presented in Eq. (1), the values of the intercept $\log\bar{a}$, inverse slope m, SD and R^2 were quantified and are summarised in Table 3 for the new test data, with separate mean stress values and all together, and the combination of the existing and new test data sets. It is worth noting that for two new data points obtained from the tests with the mean stress of $S_m = 624$ MPa, while the intercept of the mean curve was found to be $\log a$=11.606, the values of $\log\bar{a}$ and SD could not be calculated due to the lack of sufficient data points at this mean stress level.

Comparing the results on M72 hot-dip galvanised threaded connections in Tables 1 and 3, it can be seen that while the inverse slope of the S-N curve obtained from the new data varies between $m = 1.85$ for 202 MPa mean stress level and $m = 2.95$ for 624 MPa mean stress level with $m = 2.00$ for all new data points, the combination of the literature and new test data points results in an increased inverse slope of $m = 2.32$, which is smaller than the value of $m = 3$ recommended in standards for the range of N values obtained from these tests. Also seen in Table 3 is that the value of R^2 obtained from the line of best fit made to all new data points is much smaller than one. This is thought to be due to the fact that two different values of mean stress were employed in fatigue testing of M72 threaded connections in the present study. Also, it can be seen in Table 3 that the value of SD, hence the level of scatter, increases when the combination of the literature data and new data is employed in the analysis. This could be due to the fact that the literature data on M72 hot dip galvanised bolts in (Johnston and Doré, 2021) were obtained from the tests at relatively high mean stress value of $S_m = 630$ MPa, which is very close to the mean stress of 624 MPa employed in fatigue testing of two M72 studs in the present study while the remaining of the tests in the current study were performed at much lower mean stress value of 202 MPa. Therefore, combining the fatigue data points obtained at noticeably different mean stress levels has results in enlarged scatter and higher value of SD when the existing and new data on M72 threaded connections were analysed altogether. It is also worth highlighting that while the fatigue behaviour of threaded connections in bolts and studs are generally assumed to be the same, the results in Fig. 5(b) show that better fatigue lives are obtained from the new tests on M72 studs compared to the literature data on M72 bolts. Knowing that brand new bolts and studs without any prior load history were employed in the past and current studies, respectively, this might be associated with differences in thread manufacturing route of the existing and new M72 threaded connections.

Finally, yet importantly, it can be observed in Fig. 5(b) that while all of the existing and new data points fall above thickness corrected fatigue design curves from all three standards considered in this study, the mean-2SD line obtained from the regression analysis on the combination of the literature and new test data partially falls below the thickness corrected fatigue design curves of Class FAT 50 in Eurocode 3 EN 1993–1–9:2005 (EN 1993-1-9 2005) and Class G in DNV–RP-C203 (DNV-RP-C203 2021) at low values of stress range values. Likewise, if the obtained trend from the mean-2SD line was extrapolated to lower values of stress range it would have also fallen below the fatigue design curves from Class X-20 % in BS 7608 standard (BS 7608 2015). This observation indicates that for M72 threaded connections even the most conservative thickness corrected design curve among the three standards considered in this study may not conservatively predict the fatigue life of larger threaded connections, particularly in the low stress range region. This is mainly due to the steep trend with the inverse slope of $m = 2.32$ obtained from the combination of existing and new data points, compared to the inverse slope of $m = 3$ which is recommended in standards for low and medium cycle fatigue. This also highlights an important gap in the knowledge about the upper limit validity criteria for the thickness correction factors recommended in international

standards. These results suggest that more tests specially on larger threaded connections at lower stress ranges must be conducted in future work to generate a larger population of data points for more reliable statistical analysis and accurate evaluation of thickness correction factors for design of large-scale threaded connections.

3.3. Fractography analysis

Upon completion of the fatigue tests, fractography analysis was carried out by inspecting the fracture surface of each tested stud to examine the crack initiation and propagation locations. Fig. 6 presents the recreated fractography map of all seven M72 studs which were tested under fatigue loading condition in this study. The crack initiation sites have been reported with black arrows and the red arrows indicate the direction of the crack propagation. While the fatigue planes demonstrated a smooth surface due to transgranular crack growth mechanism, the fast fracture regions could be distinguished with cup and cone features which are shown in green. The fractography analysis of the studs show that in all seven samples the crack initiation and propagation occurred at the first engaged thread with the exception of M03 which showed a more complex fracture morphology. Similar to the fractography observations reported in the literature, shear lips were present on the fracture surface of all of the examined samples (González-Velázquez, 2018). In order to evaluate the dominance of fatigue failure mechanism in the tested M72 studs, the ratio of the fast fracture area over the total cross sectional area, A, was calculated for each of the tested studs following the procedure described in (ASM Handbook Commitee 1987) and the results are summarised in Table 4. The only exception was M03 which was not analysed due to the complexity of the fracture surface.

As illustrated in Fig. 6, all of the examined samples presented multiple crack initiation sites at the outer surface of the bolt. Moreover, secondary initiation points were detected using the beach marks evident on the fracture surface of M01, M02, M05 and M07 studs, which could indicate the coalescence of multiple crack planes. The fractography analysis confirms that in all of the examined samples the cracks initiate at the root of the first engaged thread at multiple locations and propagate towards the core of the bolt. Each of the crack initiation sites in the examined samples were followed by a crack propagation plane and as the tests continued of the major crack planes became dominant by absorbing the smaller planes. Moreover, the analysis of the fracture surfaces in Table 4 shows that fatigue was the dominant failure mechanism in all of the samples examined in this study with fast fracture occurring after 49–78 % of the cross-sectional area was covered by fatigue crack planes.

Table 4
The ratio of fast fracture area over cross-sectional area in M72 studs.

Sample	% fast fracture area (A_f)
M01	34
M02	33
M03	N/A
M04	18
M05	51
M06	31
M07	22

4. Analysis of the mean stress effect on fatigue behaviour of M72 threaded connections

In order to investigate the mean stress effect on the obtained results from uniaxial fatigue tests on M72 studs, the stress distributions in the threaded connections need to be analysed first. Therefore, in this section numerical analyses were initially carried out and subsequently the results from numerical simulations were employed to implement the mean

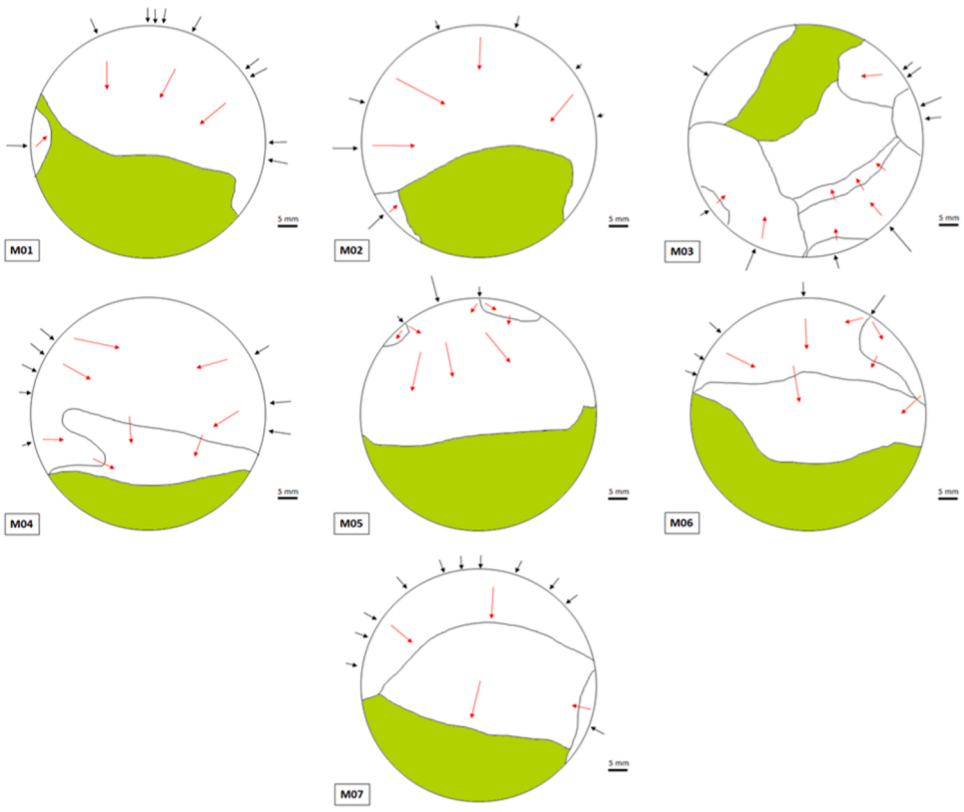

Fig. 6. Fractography results for seven M72 studs tested in the present study (the black arrows illustrate the crack initiation sites, the red arrows indicate the fatigue crack propagation direction, and the fast fracture region is shown in green).

stress correction for more accurate interpretation of the fatigue test results.

4.1. Finite element analysis

Finite element simulations were carried out to investigate the impact of the applied mean stress on the stress distribution along the engaged threads. The primary focus of this analysis was to estimate the variations in stress levels at the interface between the stud and the nut. As demonstrated in the literature (e.g. (Redondo and Mehmanparast, 2020; Chen and Shih, 1999)), the stress distribution along the engaged threads in threaded connections can be obtained in much shorter timescales and with high level of accuracy by performing simulations on a 2D axisymmetric model. Therefore, in this study a 2D axisymmetric stud-nut configuration was created in ABAQUS finite element software package by employing M72 × 6 threads in accordance with ANSI/ASME B1.13M-1995, as shown in Fig. 7. Elastic-plastic simulations were performed by assigning grade 10.9 and 8.8 steel mechanical properties to the stud and the nut, respectively, taken from the tensile curves available in the literature (see (Redondo and Mehmanparast, 2020)), with the key tensile properties of yield stress Rp,0.2,nom (which is often taken as 0.2 % proof stress of the material) and ultimate tensile strength (UTS) reported in Table 5. As seen in this table, in a threaded connection the nut is often made of a softer material with lower yield stress to facilitate the embedment of the threads during the tightening process. In order to apply the tensile load on the threaded connection, the nut geometry was fixed, by applying zero displacement and rotation boundary conditions, and a body force was applied on the stud. The interaction between the nut and the stud was defined using the tangential behaviour contact propriety with a friction coefficient of 0.15. The mesh type used for the nut and stud configuration was 3-node linear axisymmetric triangle (CAX3) and a mesh sensitivity analysis was performed to refine the mesh size to approximately 0.5 mm which was found as the optimum element size for these simulations.

A series of numerical simulations was carried out by applying various load levels equivalent to 10 %, 20 %, 50 %, 60 %, 66 %, 90 % and 100 % of the yield stress (YS) of the stud material. An example of the stress distribution results obtained from numerical simulations is shown in Fig. 8 where the applied load level was equivalent to 50 % of the YS. For each of the applied load levels, the SCF for the first 10 engaged threads was evaluated by employing the von Mises stress values to account for the spiral geometry of the threads. In order to analyse the extent of plasticity along the engaged threads, the results have been presented by classifying them into elastic (i.e. below yield stress of the material), plastic (i.e. above the yield stress of the material) and failure (i.e. above UTS) categories. As seen in Fig. 9, the first engaged thread demonstrates the highest value of SCF both in the absence and presence of plastic strains. Moreover, it can be seen that with an increase in the applied load level the extent of plasticity in the first engaged thread increases and goes beyond UTS in the case of high loads equivalent to 90 % and 100 % of the yield stress of the stud. Also seen in this figure is that the value of SCF at the first engaged thread is the highest when the deformation is purely elastic (i.e. corresponding to a stress level below yield), and it

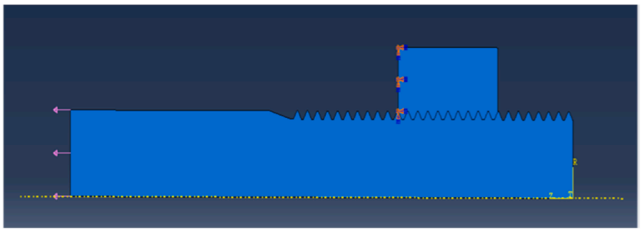

Fig. 7. Illustration of the finite element model for a 2D axisymmetric threaded connection.

Table 5
Key tensile proprieties for grade 10.9 and 8.8 steel.

	Material Type	Yield Stress (MPa)	UTS (MPa)
Nut	8.8	640	810
Stud	10.9	940	1040

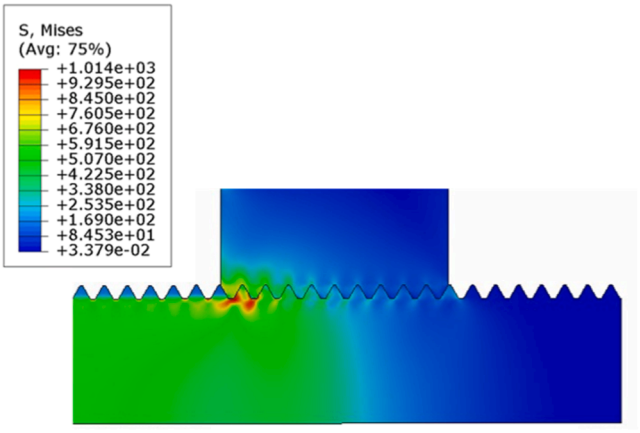

Fig. 8. Stress distribution for M72 × 6 thread connection obtained from 2D axisymmetric FEA model under 50 % YS under tension.

continually decreases as the applied load level and subsequently the extent of plastic deformation increases in the threaded connection. An important observation that can be made from these results is that while the SCF is known to be a geometry dependent factor, it is significantly sensitive to the presence or absence of plastic deformation. Similar results have been reported in the literature (Zhang et al., 2020), showing how the stress distribution and SCF change in the presence of plasticity in accordance with the applied load level. The final observation in Fig. 9 that while the number of engaged threads with plastic deformation increases by increasing the applied load, the ninth and the tenth engaged threads remain elastic even when a stress value equivalent to the yield stress of the stud material is applied in the simulation.

4.2. Mean stress correction

The influence of mean stress on the fatigue behaviour of engineering materials can be evaluated using the Goodman approach, which correlates the stress amplitude S_A with the fatigue endurance limit S_L, the mean stress S_m and the ultimate tensile stress S_{UTS} according to the following equation:

$$S_A = S_L\left(1 - \frac{S_m}{S_{UTS}}\right) \tag{3}$$

In order to evaluate the mean stress effect on the fatigue life of the M72 threaded connections, the results obtained from the present study at two different values of mean stress have been analysed using the Goodman approach. As seen in Table 5, the ultimate tensile strength for grade 10.9 steel threaded connections can be taken as $S_{UTS} = 1040$ MPa; however, the exact value of the fatigue endurance limit S_L for the examined grade of steel and stud size is unknown. Therefore, the Goodman equation in the normalised form was employed to analyse the relative mean stress effects on the fatigue life in accordance with the following equation:

$$\frac{S_{A_2}}{S_{A_1}} = \frac{\left(1 - \frac{S_{m_2}}{S_{UTS}}\right)}{\left(1 - \frac{S_{m_1}}{S_{UTS}}\right)} \tag{4}$$

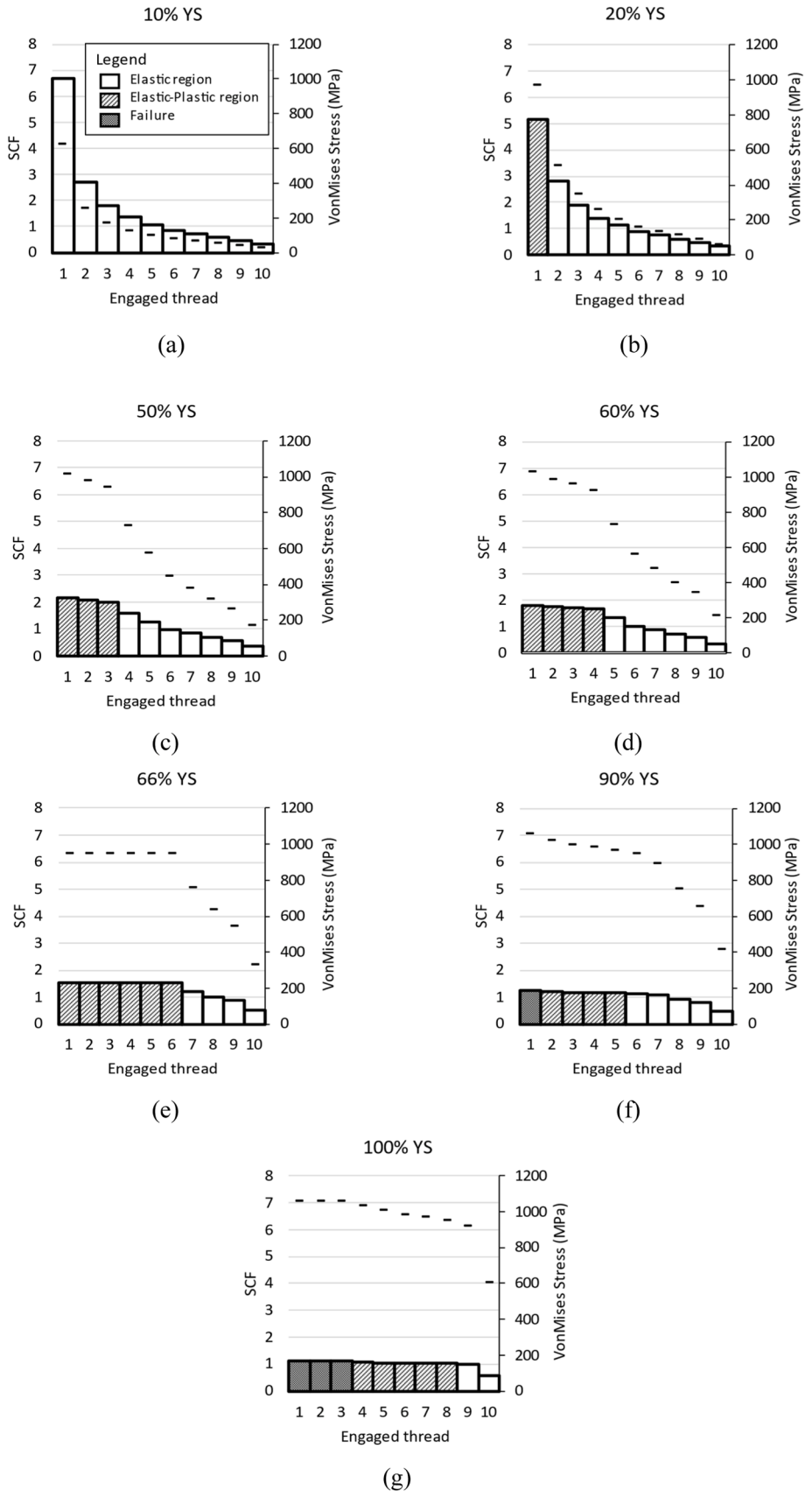

Fig. 9. Variation of the SCF value in the first 10 engaged threads under a range of applied load levels and relative von Mises stress (dash).

where S_{m_1} is the first mean stress value employed in the present study (S_{m_1} = 202 MPa), S_{m_2} is the second mean stress value, S_{A_1} is the stress amplitude corresponding to S_{m_1} and S_{A_2} is the stress amplitude corresponding to S_{m_2}. As seen in Eq. (4), the Goodman analysis allows calculating the equivalent stress amplitude that would produce the same fatigue life as S_{m_1} at a different mean stress of S_{m_2}.

Considering that S_A is half of the stress range S (or S_r), the mean fit to the fatigue data at S_{m_1} = 202 MPa was employed to predict the relative S-N fatigue behaviour at S_{m_2} at 470, 564, 624 and 658 MPa, which correspond to 50 %, 60 %, 66 % and 70 % of the yield stress of the material, receptively, using Eq. (4). The results from this analysis are shown in Table 6 and Fig. 10. As seen in Table 6, a wide range of mean stress values were considered in this study to initially investigate the gradual change in the fatigue life as a result of the increase in the mean stress value, and subsequently evaluate the accuracy of the predicted fatigue lives at S_{m_2} = 624 MPa at which two data points are available from new experiments presented in this study. It can be seen in Table 6 and Fig. 10 that an increase in the mean stress value leads to a reduction in the intercept of the mean curve log a while the inverse slope m remains unchanged. This indicates that increasing the mean stress continuously decreases the fatigue life of the threaded connections. Finally seen in Fig. 10 is that while shorter fatigue lives are predicted for higher mean stresses using the Goodman approach, the prediction line for the mean stress of 624 MPa is overly conservative compared to the two data points available at this mean stress.

According to the procedure described in (Johnston, 2022), the Goodman predictions can be modified and improved by employing the SCF value at the first engaged thread, and defining a modified stress amplitude S_A^* using the following equation:

$$S_A^* = S_A \times SCF \tag{5}$$

According to stress distribution results at various applied load levels obtained from finite element simulations demonstrated in Fig. 9, the SCF values obtained at the first engaged thread under 202 MPa (i.e. which is equivalent to ≈ 20 % of the yield stress) and 624 MPa (i.e. which is equivalent to 66 % of the yield stress) mean stress levels are found to be approximately 5 and 1.5, respectively. By incorporating the SCF value corresponding to the estimated mean stress of S_{m_2} (i.e. SCF=1.5) using Eq. (5) in conjunction with the Goodman analysis in Eq. (4), a modified Goodman prediction can be obtained the results of which are presented in Fig. 11 and Table 7. These results show that for the two experimental data points on M72 studs tested at the mean stress of 624 MPa, the Goodman method introduces a significant percentage of error ranging between 37 % and 45 % with a high degree of under prediction. However, using the modified Goodman method the predicted points fall very close to the experimental data points, significantly reducing the percentage of error to much lower values ranging between 5 % and 18 %. This analysis confirms that the employment of the SCF value of 1.5 at the first engaged thread obtained at the mean stress value of equivalent to 66 % of the yield stress of the stud material results in satisfactory predictions of the fatigue trends at this mean stress level using the modified Goodman approach.

Further investigations need to be carried out in future work by conducting more fatigue tests on large-scale M72 threaded connections as well as employment of a wider range of mean stress correction approaches to better understand the design, life prediction and structural integrity analysis of large-scale bolted connection in offshore wind turbines. Moreover, further numerical analysis will need to be carried out to thoroughly investigate the bolt size effects on the fatigue life and durability of threaded connections in offshore renewable energy structures.

Table 6
Goodman predictions at different mean stress values.

Mean stress (% of yield)	m	log$a$
50	1.85	9.131
60	1.85	8.986
66	1.85	8.884
70	1.85	8.809

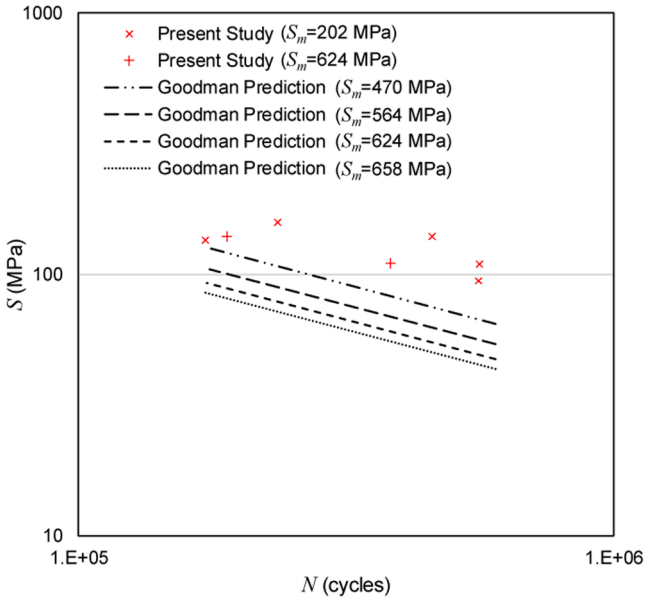

Fig. 10. Comparison of the experimental data with Goodman prediction lines at different mean stress values.

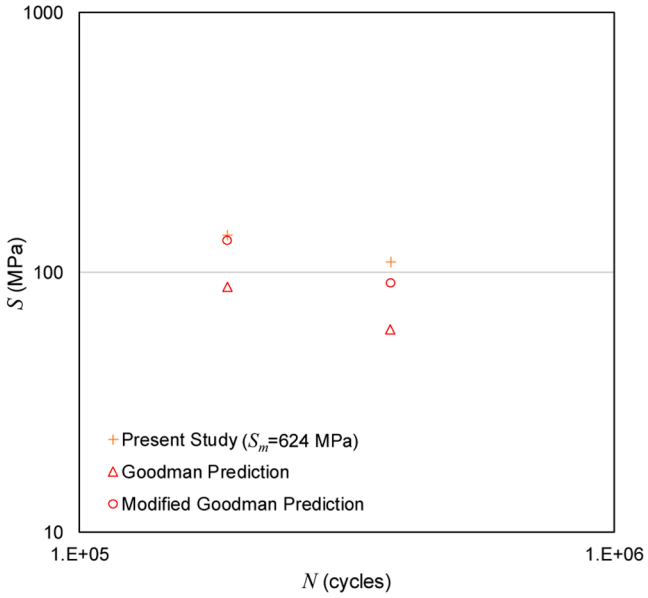

Fig. 11. Comparison of the Goodman and modified Goodman predictions with the experimental data on M72 studs at mean stress of 624 MPa.

Table 7
Calculation of percentage of error in Goodman and modified Goodman predictions for two experimental data points at mean stress of 624 MPa.

N	S (experimental)	S (Goodman)	Error	S (Modified Goodman)	Error
3.82×10^5	111	61	45 %	91	18 %
1.89×10^5	141	89	37 %	133	5 %

5. Conclusions

This paper presents the findings from a comprehensive study of the fatigue behaviour in threaded connections by firstly, assessing the S-N fatigue behaviour of medium to large size bolts using the data available in the literature, and secondly, evaluating the fatigue behaviour of M72 hot dip galvanised threaded connections, which are widely used in offshore wind turbines, by performing new large-scale tests. The analysis of the existing data points on M36, M48, M64 and M72 galvanised threaded connections in the literature shows that while the dominant majority of data points fall above the fatigue design curves recommended by all three standards, a steep inverse slope of $m < 3$ for mean-2SD line can lead the experimental trend to fall below the recommended thickness corrected design curves particularly at lower stress ranges. Further contribution to knowledge has been made in this study through numerical and experimental investigation of large-scale M72 threaded connections loaded under tension. The results from new tests on M72 studs at two different mean stress values of 202 MPa and 624 MPa confirm that the inverse slope of the fatigue design curve in large-scale threaded connections can be considerably lower than three, but more test data are needed to confirm this observation. Moreover, the numerical analysis of the stress variation across the engaged threads shows that the highest value of stress concentration factor is always found to be at the first engaged thread and this value continuously decreases by increasing the applied load level and introducing local plasticity in the threaded connections. Finally, it has been shown that the application of the modified Goodman correction successfully corrects for the effect of different mean stress levels used in the tests, and highlights the need to correct for mean stress when combining test data from threaded connections tested at different mean stress levels.

CRediT authorship contribution statement

Alessandro Annoni: Writing – original draft, Validation, Methodology, Investigation, Formal analysis. **Carol Johnston:** Writing – review & editing, Validation, Resources, Methodology, Conceptualization. **Ali Mehmanparast:** Writing – review & editing, Supervision, Methodology, Funding acquisition, Conceptualization.

Declaration of competing interest

The authors declare that they have no known competing financial interests or personal relationships that could have appeared to influence the work reported in this paper.

Acknowledgements

This work was supported by grant EP/L016303/1 for Cranfield, Oxford, and Strathclyde Universities Centre for Doctoral Training in Renewable Energy Marine Structures – REMS CDT (http://www.rems-cdt.ac.uk/) from the UK Engineering and Physical Sciences Research Council (EPSRC). The authors would like to acknowledge the technical support at TWI for performing large-scale fatigue tests on M72 studs.

References

ASM Handbook Commitee, Fractography, 1987.
Braithwaite, J., Mehmanparast, A., 2019. Analysis of tightening sequence effects on preload behaviour of offshore wind turbine M72 bolted connections. Energies. (Basel) 12 (23), 4406.
Braithwaite, J., Goenaga, I.G., Tafazzolimoghaddam, B., Mehmanparast, A., 2020. Sensitivity analysis of friction and creep deformation effects on preload relaxation in offshore wind turbine bolted connections. Appl. Ocean Res. 101, 102225.
BS 7608, 2015. Guide to Fatigue Design and Assessment of Steel Products, Edition 2014+A1. British Standards Institution.
Charlton, R.S., 2011. Threaded fasteners: part 1-Failure modes and design criteria of connections. In: NACE CORROSION (pp. NACE-11164). NACE.
Chen, J.J., Shih, Y.S., 1999. A study of the helical effect on the thread connection by three dimensional finite element analysis. Nucl. Eng. Des. 191 (2), 109–116.
DNV-RP-C203: Fatigue design of offshore steel structures, Det Norske Veritas, Edition 2021-09.
EN 1993-1-9, 2005. Eurocode 3: Design of Steel Structures - Part 1-9: Fatigue. Comité Européen de Normalisation, Brussels, Belgium.
González-Velázquez, J.L., 2018. Fractography and Failure Analysis, 24. Springer International Publishing, Switzerland.
HM Government, The ten point plan for a green industrial revolution. 2020.
Johnston, C., Doré, M., 2021. Comparison of the fatigue performance of galvanised M72 bolts with design standard recommendations. In: Proceedings of the International Conference on Offshore Mechanics and Arctic Engineering, OMAE2021- 62758. American Society of Mechanical Engineers.
Johnston, C., 2022. Effect of low pretension on the fatigue performance of large bolts. In: Proceedings of the International Conference on Offshore Mechanics and Arctic Engineering, OMAE2022-78556. American Society of Mechanical Engineers.
Lochan, S., Mehmanparast, A., Wintle, J., 2019. A review of fatigue performance of bolted connections in offshore wind turbines. Procedia Struct. Integrity 17, 276–283.
Lotsberg, I., Serednicki, A., Bertnes, H., Lervik, A., 2012. Design of grouted connections for monopile offshore structures. Stahlbau 81 (9), 695–704.
Mang, F., Herion, S., Fleischer, O., Koch, E., 2003. Untersuchung von Zug-Druck-Kalottenlagern im Großversuch (in German). Stahlbau 72 (1), 43–49.
Mehmanparast, A., Lotfian, S., Vipin, S.P., 2020. A review of challenges and opportunities associated with bolted flange connections in the offshore wind industry. Metals. (Basel) 10 (6), 732. Vol. 10, Page 732.
Redondo, R., Mehmanparast, A., 2020. Numerical analysis of stress distribution in offshore wind turbine M72 bolted connections. Metals. (Basel) 10 (5), 689. Vol. 10, Page 689.
Schaumann, P., Eichstädt, R., 2016. Ermüdung sehr großer HV-Schraubengarnituren (in German). Stahlbau 85 (9), 604–611.
Schaumann, P., Eichstädt, R., 2018. Experimental and analytical fatigue assessment of high-strength bolts for wind turbine structures. In: Proceedings of the Conference: Kolloquium zum, 60.
Schaumann, P., Eichstädt, R., Oechsner, M., Simonsen, F., 2015. Ermüdungsfestigkeit feuerverzinkter HV-Schrauben in Ringflanschverbindungen von Windenergieanlagen. Stahlbau 84 (12), 1010–1015.
Schaumann, P., F. M.-P., 2009. Fatigue resistance of high strength bolts with large diameters. In: Proceedings of the International Symposium for Steel Structures ISSS. Seoul, Korea, pp. 12–14.
Seidel, M., Schaumann, P., 2001. Ermittlung der Ermüdungsbeanspruchung von Schrauben exzentrisch belasteter Flanschverbindungen. Stahlbau 70 (7), 474–486.
Stranghöner, N., Abraham, C. and Jungbluth, D., Preloading procedures to achieve a reduced preloading level in the elastic range of the bolt material with sufficient reliability. Deliverable report D1.5 (WP 1 – Task 1.5), 2018.
Tougher, S., Foyer, J., Morena, E., 2017. Globalising the climate: COP21 and the Climatisation of Global Debates. Taylor & Francis.
Ungermann, D., Rademacher, D., Oechsner, M., Simonsen, F., Friedrich, S., Lebelt, P., 2015. Feuerverzinken im Brückenbau (in German). Stahlbau 84 (1), 2–9.
Unglaub, J., Reininghaus, M., Thiele, K., 2015. Zur Ermüdungsfestigkeit von feuerverzinkten Zugstäben mit Endgewinden. Stahlbau 84 (8), 584–588.
Zhang, D., Wang, G., Huang, F., Zhang, K., 2020. Load-transferring mechanism and calculation theory along engaged threads of high-strength bolts under axial tension. J. Constr. Steel. Res. 172, 106153.